Ecological Indicators 153 (2023) 110431

Contents lists available at ScienceDirect

Ecological Indicators

journal homepage: www.elsevier.com/locate/ecolind

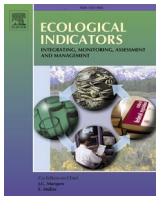

The seeds of ecological recovery in urbanization – Spatiotemporal evolution of ecological resiliency of Dianchi Lake Basin, China

Donghui Li [a,1], Junming Yang [a,1], Tianzi Hu [b,1], Guifang Wang [c], Samuel A. Cushman [d], Xinyu Wang [c], Kollányi László [c], Rui Su [a], Lifei Yuan [a], Bingpeng Li [a], Yawen Wu [a,*], Tian Bai [a,*]

[a] College of Landscape and Horticulture, Yunnan Agricultural University, Kunming 650201, China
[b] School of Landscape Architecture, Beijing University of Agriculture, Beijing 102206, China
[c] Institute of Landscape Architecture, Urban Planning and Garden Art/Hungarian University of Agriculture and Life Sciences, Budapest, Hungary
[d] Department of Biology, University of Oxford, Oxford, UK

ARTICLE INFO

Keywords:
Ecological resiliency evaluation
Entropy weight TOPSIS
Barycenter migration
CA-MC
Dianchi Lake basin

ABSTRACT

As a result of years of monitoring the ecological resiliency of natural areas and cities, it has become clear that it is both important and often feasible to implement ecological and environmental restoration in conjunction with ongoing processes of landscape change development and urbanization. Ecological resiliency and spatiotemporal evolution studies can objectively reveal the resiliency of ecosystems to external disturbances. Ecological monitoring and assessment can also help planners understand regional ecological spatial differentiation patterns and provided data support for planning. In this paper we have analyzes quantitatively the interrelationships of ecological factors in Dianchi Lake Basin (DLB) over the past 30 years and explored the spatial and temporal dynamics of ecological resiliency. Based on remote sensing images and primary data in 1995, 2005, 2010, 2015, 2018, and 2022, we used the center of gravity migration and kernel density analysis to explore the spatial and temporal changes of ecological resiliency. We built the overall resiliency evaluation system using entropy weight in the TOPSIS model, and finally simulate the future changes based on CA-Markov (CA-MC) model. The results show that from 1995 to 2022, the ecological resiliency of land use and vegetation cover in DLB decreased substantially. An important finding was that the ecological resiliency of riparian buffer zone and landscape pattern were generally increasing. The distribution of barycenter movement and kernel density of different levels of ecological resiliency differed significantly and showed fluctuating changes. The extreme low resiliency and extremely resilient areas shift to the northeast, the mildly resilient areas shift to the northwest, and the highly resilient areas shift to the southeast. The overall resiliency level of DLB is predicted to slowly increase from 2022 to 2030 by deduction of the CA-MC model. Our analysis suggests that the study of the evolution of regional ecological resiliency can provide a timely understanding of regional ecological evolution patterns and propose ecological protection strategies.

1. Introduction

The rapid development of urbanization has led to the reduction of the extent and function of ecosystems and excessive disturbance of ecological processes. As a result, ecological security problems such as reduced vegetation, soil erosion, deterioration of riparian buffer zones and loss of biodiversity have become common (Duan et al., 2021; Ma et al., 2004; Jin et al., 2020). The concept of Ecological resiliency is the ability of complex systems to resist severe stress and restore their original state which can describe their changes through multiple indicators. It plays a vital role in guiding regional environmental protection and spatial planning, and evaluating regional ecological security resiliency (Zhang et al., 2010; Chow and Sadler, 2010). Thus, ecological resiliency has scientific reference value for formulating regional ecological, environmental protection and restoration management measures (Yu et al., 2020). GIS analysis of watershed ecological resiliency is essential for

* Corresponding authors.
E-mail addresses: landsliy@ynau.edu.cn (D. Li), 742891286@qq.com (J. Yang), 202230511003@bua.edu.cn (T. Hu), wgf0317@163.com (G. Wang), sam.cushman@gmail.com (S.A. Cushman), sdwangxinyuxw@126.com (X. Wang), kollanyi.laszlo@uni-mate.hu (K. László), yawenwu@ynau.edu.cn (Y. Wu), tbai@ynau.edu.cn (T. Bai).
[1] Co-first authors.

https://doi.org/10.1016/j.ecolind.2023.110431
Received 28 February 2023; Received in revised form 17 May 2023; Accepted 25 May 2023
Available online 10 June 2023

regional environmental research and continues to innovate. With traditional evaluations gradually evolving into coupled models, it is increasingly important that GIS can reveal the characteristics of ecological resiliency patterns and processes from multiple perspectives (Shi et al., 2018; Chi et al., 2019; Chambers et al. 2019; Cushman and McGarigal, 2019). Markov chain (MC) and cellular automata (CA) are both time-discrete and state-discrete dynamical models. The coupled CA-MC model draws on the advantages of both to achieve long-term prediction of the spatial evolution of complex systems and has been widely used in ecological research with promising results (Mondal et al., 2016; Adhikari and Southworth, 2012; Aburas et al., 2017).

DLB is located the core area of the central Yunnan urban agglomeration. Its ecological environment has been dramatically impacted by urbanization, population dramatic increase and the most important reclamation. An application of scientific methods to investigate the quantitative traits and spatial evolution of ecological resiliency in the DLB would help promote its governance, protection, and sustainable development (Duan et al., 2021; Wang et al., 2021). This paper provides an overview and integration of the use of resiliency concepts to guide natural resources management actions. We emphasize ecosystems and landscapes and provide examples of the use of these concepts from empirical research in applied ecology. We begin with a discussion of definitions and concepts of ecological resiliency and related terms that are applicable to management. We suggested that a resiliency-based management approach facilitates regional planning by providing the ability to locate management actions, used the Entropy Weight TOPSIS (Technique for Order Preference by Similarity to an Ideal Solution) method and CA-MC model to combine static evaluation and dynamic prediction. These methods are more objective than the traditional AHP, MSE and AHP-GIS methods. We used the 2920 km^2 extent of the DLB as the study area (Civco, 1993; Baqa et al., 2021; Mokarram et al., 2021). Based on data charting in the study area from 1995 to 2022, we used the CA model in combination with the Markov model to predict and map ecological resiliency change for 2026 and 2030. Specific objectives of the work were to: (1) calculation, evaluation and compare ecological resiliency changes from 1995 to 2022 in DLB; (2) predict and map ecological resiliency changes in 2026 and 2030 in DLB. (3) Providing countermeasures and recommendations for the future development planning of DLB based on the experimental results.

2. Research material

2.1. Study area

The DLB (24°28′ ~ 25°28′ N, 102°30′ ~ 103°00 E) is part of the Yangtze River basin and the Jinsha River system, and is important to conservation,because it provides high regional ecological diversity at the scale of central Yunnan (Fig. 1). Since the 1960s, the ecological environment of DLB has suffered extensive ecological deterioration. After 30 years of treatment, the water quality of Dianchi is still mainly V (Surface water environmental quality standard GB 3838–2002, China, waste water of worst quality), with some rivers of IV (Surface water environmental quality standard GB 3838–2002, China, Non-human contact waste water, only better than class V), and algal blooms occur frequently in summer. It is one of the most polluted lakes in China (Zhang et al., 2014; Li et al., 2019; Huang et al., 2014). The destruction

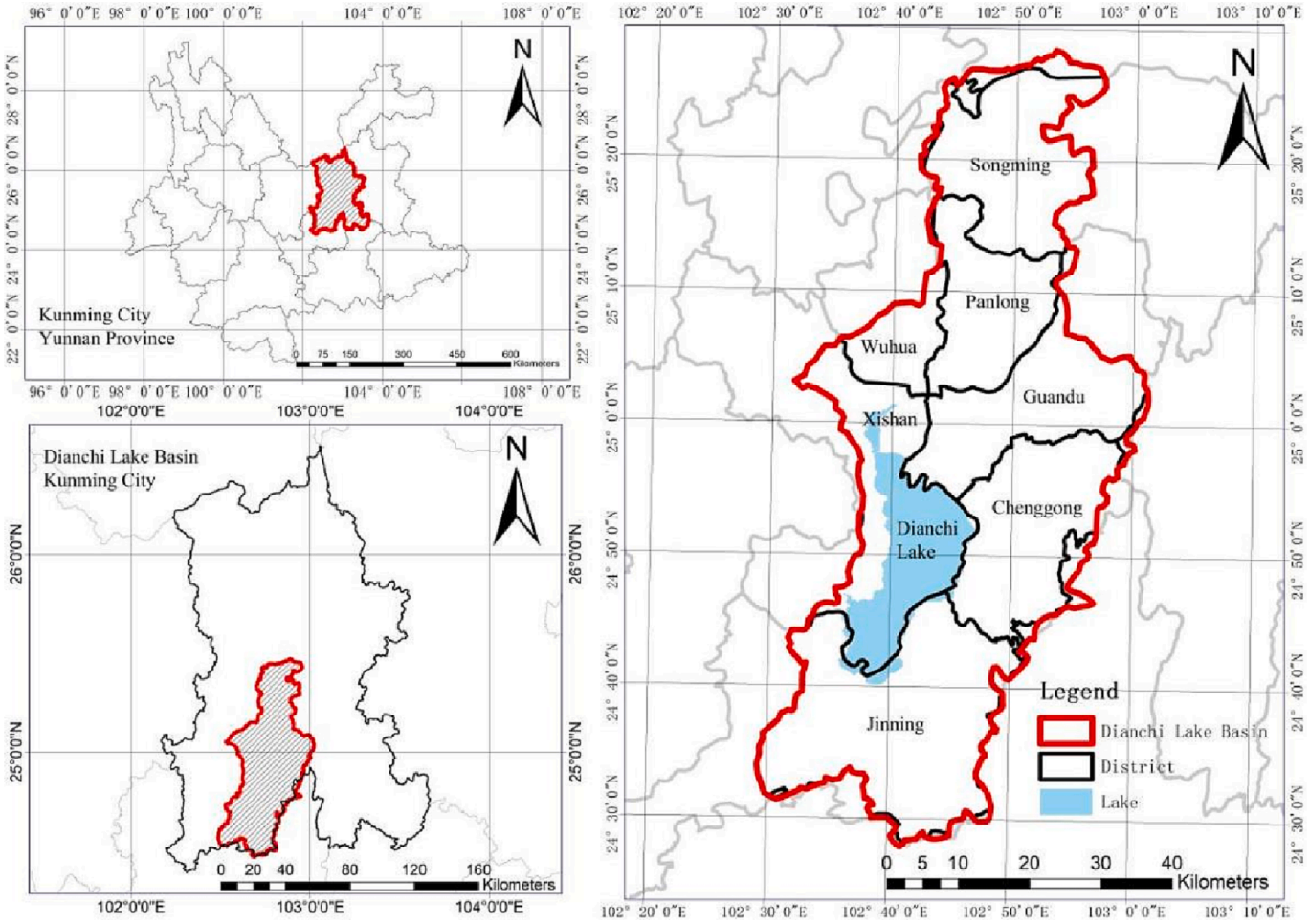

Fig. 1. Research area overview Note: the study area is the Yunnan-Guizhou Plateau in southwest China.

and degradation of vegetation in the DLB continues to occur. Forest cover in the basin was maintained at around 25% since 1974 until approximately 2006 (Niu et al., 2015).

Since 2006, the project of relocation of people, houses and farmland, restoration of ponds, lakes, water park reserves and wetlands has been carried out in Dianchi, and the environmental quality has been steadily improved, with the forest cover rebounding to 40.78% in 2017. Plant cover and species diversity have increased, and the ecological environment has gradually improved (Niu et al., 2015; Luo et al., 2018). However, the vegetation cover of DLB is still lower than the level of national targets (Hou et al., 2016; Li et al., 2021).

2.2. Data source

Data obtained spatial correction, geographic alignment, and supervised classification based on Landsat 4–5 TM and Landsat 8 OIL_TIRS 30 m remote sensing images and Digital Elevation Model (DEM) in 1995, 2005, 2010, 2015, 2018 and 2022. Four ecological resiliency factors and sub-indicators were sorted and screened out by TOPSIS sorting method among multiple factors, and the ecological resiliency of the comprehensive DLB was evaluated. These factors specifically are: land use and cover change (LUCC), normalized difference vegetation index (NDVI), riparian buffers (RB), and landscape pattern index (LPI) (Lu et al., 2023; Wei et al., 2023) (Table 1).

3. Method

3.1. Basin evaluation index system

Based on the geospatial database, we established an ecological resiliency index system with reference to relevant literature (Kazanci et al., 2023), including LUCC, DEM, NDVI, RB and LPI factors indexes and sub-indexes (Li et al., 2021). LPI factors can quantify the current state of the landscape pattern and make the evaluation of ecological restoration in the study area more scientific (Wang et al., 2014). We excluded indices with relatively similar expression of results, and selected four relevant landscape indices to describe the landscape characteristics at a county level. largest patch index (LPI), average patch area (AREA_MN), shannon's diversity index (SHDI), shannon's evenness index (SHEI), were selected as LPI factors to show the degree of spatial variability (Hu et al., 2023); shannon's diversity Index (SHDI) and shannon's evenness index (SHEI) as fitted data, reflected the change of regional information quantity (Wang et al., 2022; Zhao and Huang, 2022); weighted with LUCC, NDVI, and RB factors (Deng et al., 2022).

According to the resiliency factor superimposed efficacy and contribution rate, the evaluation factors were divided into resiliency classes (Zhou and Li, 2015; Chen and Wu, 2020). The study area was classified into five classes: extremely high resiliency, high resiliency, moderate resiliency, low resiliency, and extreme low resiliency areas (Table 2).

Table 1
Principal data sources.

Abbreviation	Source	Resolution	Operation
LUCC	Resource and environment science data center of Chinese Academy of Sciences	30 m	Rasterize
NDVI	Geospatial data cloud landsat4-5 TM	30 m	
RB	satellite digital product, landsat8 OIL_TIRS satellite digital product	30 m	
DEM	the Shuttle Radar Topography Mission (SRTM)	30 m	
LPI	Resource and environment science data center of Chinese Academy of Sciences	30 m	

3.2. Impact factor weight analysis

3.2.1. The entropy method

In the past, many articles on evaluation used subjective evaluation, such as the application of Analytic Hierarchy Process (AHP) in landscape research (Ma et al., 2022; Yin et al., 2022). However, we hope to obtain the weight of the resiliency of the evaluation region by calculating the change of information in each region, and take the degree of change as the evaluation basis. Here, we used entropy value can be used to analyze the change of environmental information quantity to objectively obtain the weight of recovery evaluation. The entropy method remedies a defect of the AHP hierarchical analysis method and Telfer expert evaluation method that are more subjective (Li et al., 2019; Zou et al., 2021). The basic idea of entropy weight theory is that the greater the degree of dispersion, the greater the influence of the index on the comprehensive evaluation (Zou et al., 2006; Zhang, 2009; Liu et al., 2016).The weight of the factor was determined according to the influence of the relative change of the factor on the overall system, which has strong objectivity (Huang et al., 2017; Li et al., 2015), and the steps of our implementation followed (Amiri et al., 2014; Han et al., 2015):

(1) Standardize the original value of indicators:

Positive indicators:

$$xij = \frac{xij - \min(xij)}{\max(xij) - \min(xij)} + 0.00001 xij = \frac{xij - \min(xij)}{\max(xij) - \min(xij)} + 0.00001 \tag{1}$$

Negative indicators:

$$xij = \frac{\max(xij) - xij}{\max(xij) - \min(xij)} + 0.00001 xij = \frac{\max(xij) - xij}{\max(xij) - \min(xij)} + 0.00001 \tag{2}$$

(2) Calculate the entropy value W_j of the jth indicator:

$$wj = -\frac{1}{\ln(n)} \sum_{i=1}^{n} \frac{Tij}{\sum_{i=1}^{n} Tij} \ln \frac{Tij}{\sum_{i=1}^{n} Tij} \tag{3}$$

where: W_j is the entropy value of the jth indicator, T_{ij} is the standardized data of year i in indicator j; $\frac{Tij}{\sum_{i=1}^{n} Tij}$ is the dimensionless value of each indicator after data standardization and non-negativity.

3.2.2. TOPSIS sorting method

The TOPSIS method is a commonly used comprehensive evaluation method for the comparative selection of indicators or multiple solutions. It has been widely used in recent years, in the form of applications that have calculated the weighted Euclidean distance between each candidate indicator and the ideal solution, ranking the proximity of multiple indicators, and then balancing and assessing the advantages and disadvantages of each evaluation indicator (Chang et al., 2021; Cheng et al., 2020).

Here are the steps of the TOPSIS method (Hwang and Yoon, 1981):

(1) Establish the decision matrix $R = \{r_{ij}\}$, where r_{ij} is the value of the j^{th} attribute in the i^{th} alternative; i = 1, 2, …, m; j = 1,2, …, n.
(2) Normalize the decision matrix R and transform it to the normalized matrix

$$R' = \{r'ij\} \tag{4}$$

(3) Calculate the weighted normalized decision matrix $V = \{v_{ij}\}$

$$vij = wjr'ij \tag{5}$$

For the entropy-based TOPSIS method, the weight in Eq. (4) is calculated by the EM.

Table 2
Classification standard of ecological resiliency.

Evaluation factors	Ecological resiliency classification				
	Extreme low resiliency	Low resiliency	Medium resiliency	High resiliency	Extreme resiliency
LUCC	construction land, reserved land	cultivated land, orchard, other agricultural land	Grassland	Forest	water area
NDVI	≤0.2	0.2–0.4	0.4–0.6	0.6–0.8	> 0.8
RB (m)	≥500	350–500	200–300	100–200	<100
LPI	LPI				
LPI	AREA_MN		Each index is divided into five levels using the natural breakpoint method, respectively assigned 1, 3, 5, 7, 9		
	SHDI				
	SHEI				

(4) $A^+ = \{(\max_i vij|j \in J), (\min_i vij|j \in J')|i = 1, 2, ..., m\} = \{v_1^+, v_2^+, ..., v_n^+\}$ Determine the ideal solution A+ and the negative ideal solution A−:

$$A^+ = \{(\max_i vij|j \in J), (\min_i vij|j \in J')|i = 1, 2, ..., m\} = \{v_1^+, v_2^+, ..., v_n^+\} \quad A^+ = \{(\min_i vij|j \in J), (\max_i vij|j \in J')|i = 1, 2, ..., m\} = \{v_1^-, v_2^-, ..., v_n^-\} \tag{6}$$

$$A^+ = \{(\min_i vij|j \in J), (\max_i vij|j \in J')|i = 1, 2, ..., m\} = \{v_1^-, v_2^-, ..., v_n^-\} \tag{7}$$

J' where J = {j = 1, 2,…, n| j associated with the − bigger − the − better attribute}, = {j = 1, 2, …, n | j associated with the − smaller − the − better attribute}.

(5) $S_i^+ = \sqrt{\sum_{j=1}^n (vij - v_i^+)^2}$ Calculate the DIS and DNIS by the following equations:

$$S_i^+ = \sqrt{\sum_{j=1}^n (vij - v_i^+)^2} \tag{8}$$

$$S_i^- = \sqrt{\sum_{j=1}^n (vij - v_i^-)^2} \tag{9}$$

(6) Calculate the relative closeness of each alternative by the following equation:

$$RCi = \frac{S_i^-}{S_i^+ + S_i^-} \tag{10}$$

Finally, the evaluation schemes were ranked in descending order based on the value of RC_i, where RC_i indicates the relative closeness of the LUCC, NDVI, RB and LI factors, and the larger RC_i is, the closer the evaluation was to the positive ideal solution, indicating that the weight of this single factor was significant, and vice versa (Xu et al., 2021; Qiao et al., 2021).

3.3. Calculating the barycenter of ecological resiliency

The barycenter refers to a certain spatial point, in all directions of which the powers are relatively balanced. As an important analysis tool for studying changes of spatial patterns, the barycenter models, such as grain production barycenter, population barycenter and energy barycenter model, are also frequently used for the spatial analysis (Wang et al., 2018; Bigot and Klein, 2012; Zhang et al., 2012). The ecological resiliency barycenter is formed according to above theory. The barycentric coordinates can be calculated by the following formula:

$$x_j = \sum_{i=1}^n (T_{ij}.xi) / \sum_{i=1}^n T_{ij} \tag{11}$$

$$y_j = \sum_{i=1}^n (T_{ij}.yi) / \sum_{i=1}^n T_{ij} \tag{12}$$

$x_j = \sum_{i=1}^n (T_{ij}.xi) / \sum_{i=1}^n T_{ij}$ where, T_{ij} (i = 1, 2, 3, … n) means the grain output of the i^{th} county; P_i (x_i, y_i) is the barycentric coordinate of each county; P_j (x_j, y_j) is the national barycentric coordinate of grain output in the j^{th} year.

3.4. Kernel density estimation of ecological resiliency

Kernel density estimation (KDE) is one of the most popular methods for analyzing the first order properties of a point event distribution (Gatrell and Bailey, 1996; Silverman, 1986) because it is easy to understand and implement. Two-dimensional grayscale representation of the results of the kernel density calculation, which allows visualization of the distribution characteristics such as aggregation or dispersion of the landscape. With the help of a moving window, the point or line density of the raster cells was calculated and output (Xie and Yan, 2008; Elgammal et al., 2002). There were usually Rosenblatt-Parzen kernel estimates:

$$f_{n(x)} = \frac{1}{nh} \sum_{i=1}^n (\frac{x - x_i}{h}) \tag{13}$$

3.5. CA-MC model prediction analysis

(1) The CA model consists of four parts: the cell and its state, the cell space, the cell neighborhood, and transformation rules. Given discrete units of time, space, and state, any cell variable exists only in finite and discrete states. Our analysis was modified synchronously, according to the same transformation

regulations. The rules of state change are localized in time and space, and the ordinary CA model is:

$$S=(t+1)=f[S(t),N] \tag{14}$$

where S is the finite, discrete set of states of the tuple; N is the neighbors of the tuple; and f is the transformation rule of the locally mapped tuple.

(2) The MC model is used to calculate the spatial transformation probability, using the before and after states of temporal development to statistically explain the characteristic law of change transfer of an event in a certain period (Cui et al., 2021). The evolution of ecological resiliency was characterized by the MC process, and the gradation corresponds to the "possible states" in the MC process, and the area or ratio of the gradation to each other was the state transfer probability, which was expressed as follows.

$$N_{t+1}=N_t{}^{*}Pij \tag{15}$$

$$P_{ij}=\begin{pmatrix} P_{11} & P_{12}\cdots & P_{1n} \\ P_{21} & P_{22}\ldots & P_{2n} \\ P_{n1} & P_{n2}\ldots & P_{nn} \end{pmatrix} \tag{16}$$

$$0\leqslant Pij<1 and \sum_{i=1}^{n} Pij=1(i,j=1,2...,n) \tag{17}$$

where: N_{t+1} denotes the ecological resiliency grading in the latter period, N_t denotes the ecological resiliency grading in the former period, and P_{ij} denotes the state transfer probability matrix (Wang et al., 2018). The MC model has the characteristic of time series extrapolation, while the CA model has the advantage of predicting the spatio-temporal dynamic evolution of complex systems, so the combined two models can scientifically extrapolate the spatial changes of ecological resiliency in watersheds (Souidi et al., 2019).

In this paper, the Kappa coefficient is used to test the accuracy of the prediction of land pattern evolution. Its calculation formula is:

$$Kappa=(P0-Pc)/(Pp-Pc) \tag{18}$$

where: P_0 is the proportion of correct simulations; P_c is the proportion of correct predictions in the random case of the model; P_p is the proportion of correct predictions in the ideal case.

4. Results and analysis

4.1. Single-factor ecological resiliency evaluation

4.1.1. LUCC single factor resiliency evaluation

Ecological resiliency is the emergency response of LUCC to human disturbance, and the natural recovery ability of "elastic deformation" will gradually weaken with the increasing intensity of human intervention. Therefore, in this paper, ecological resiliency is water area > forest land > grassland > cultivated land > construction land, and the ecological resiliency is calculated with the weight of entropy (Wen et al. 2021). The results of the study (Table 3 and Fig. 2) show that the resiliency of LUCC in the DLB is high. The extremely high resiliency area was maintained at more than 10% in the past 30 years. Meanwhile, the resiliency of LUCC shows a decreasing trend from the periphery of the basin to the central city. The extremely high resiliency areas are mainly located in the central part of the basin where the river system is concentrated. In contrast, to this, the extreme low resiliency and low resiliency areas show a trend of distribution around Dianchi. Across the time series there was an overall decreasing trend in ecological resiliency in LUCC. For example, extremely high resiliency area decreased by 0.86%, while the area of moderately resilient areas increased by 12.53%. The area of urbanized and developed land increased while the LUCC resiliency decreased.

4.1.2. NDVI single factor resiliency evaluation

NDVI is divided into 5 categories according to the natural break point method. The results of the study show (Table 4 and Fig. 3) that from 1995 to 2022, the NDVI index of DLB is low, and the NDVI index is greater than or equal to 0.2 was all above 35%. The NDVI index greater than 0.8 is mainly distributed in the marginal area of the basin. In the time series study region overall, regions with NDVI index less than or equal to between 0.2, 0.4–0.6, 0.6–0.8 decreased by 0.29%, 4.27%, and 0.01%, respectively, which all shifted to regions with NDVI index between 0.2 and 0.4. Vegetation growth status is similar in 1995 and 2005, but the vegetation growth levels were higher in 2005. The 2018 NDVI index was higher than that in 2015 and 2010, and the NDVI index shows an upward trend from 2005. The NDVI index declined in 2022 compared to 2018.

4.1.3. RB single factor resiliency evaluation

The results of the study show (Table 4 and Fig. 4) that during 1995–2018, the RB resiliency level in DLB is low, and the sum of the ratio of extreme low resiliency and low-resiliency areas are above 45%. The closer the distance to the water system, the higher the region's resiliency. On the time series, the RB resiliency class in 2022 is increasing compare with 1995, with an increase of 1.47% in its highly resilient area, and 1.05% and 1.04% in the extremely and moderately resilient areas, respectively.

4.1.4. LI single factor resiliency evaluation

From our review of the relevant literature, followed up with principal component analysis, four indices were extracted from the first principal component at the landscape level: LPI, AREA_MN, SHDI, SHEI. We divided the Dianchi watershed into rectangles of 6 km × 6 km in dimension to obtain 84 vector data maps of equal magnitude, which were imported into Fragstats 4.2 (McGarigal, 2014) for the calculation of landscape pattern indices. Then the inverse distance weights and natural breakpoint method were used to obtain the four indices of ecological resiliency maps (Zięba-Kulawik et al., 2022; Lu et al., 2019). The entropy value method was used to obtain the landscape pattern index weights, and the weighted superposition was calculated to obtain the LI resiliency distribution map of Dianchi watershed from 1995 to

Table 3
LUCC resiliency of DLB from 1995 to 2018.

Region	Extreme low resiliencyarea		Low resiliency area		Moderate resiliency area		High resiliency area		Extreme resiliency area	
	Area/ km^2	Percentage/%	Area/ km^2	Percentage/%	Area/ km^2	Percentage/%	Area/ km^2	Percentage/%	Area/ km^2	Percentage/%
1995	275.07	8.96	707.13	23.04	598.06	19.48	1148.79	37.42	340.59	11.10
2005	301.93	9.84	721.24	23.51	605.45	19.73	109.71	35.75	342.79	11.17
2010	388.07	12.65	671.79	21.89	526.16	17.15	114.14	37.20	341.08	11.12
2015	410.07	13.36	659.78	21.50	519.48	16.93	113.91	37.12	340.06	11.08
2018	625.51	20.39	531.95	17.34	473.68	15.44	110.79	36.11	329.38	10.73
2022	659.35	21.49	759.32	24.74	556.60	18.14	779.35	25.40	314.32	10.24

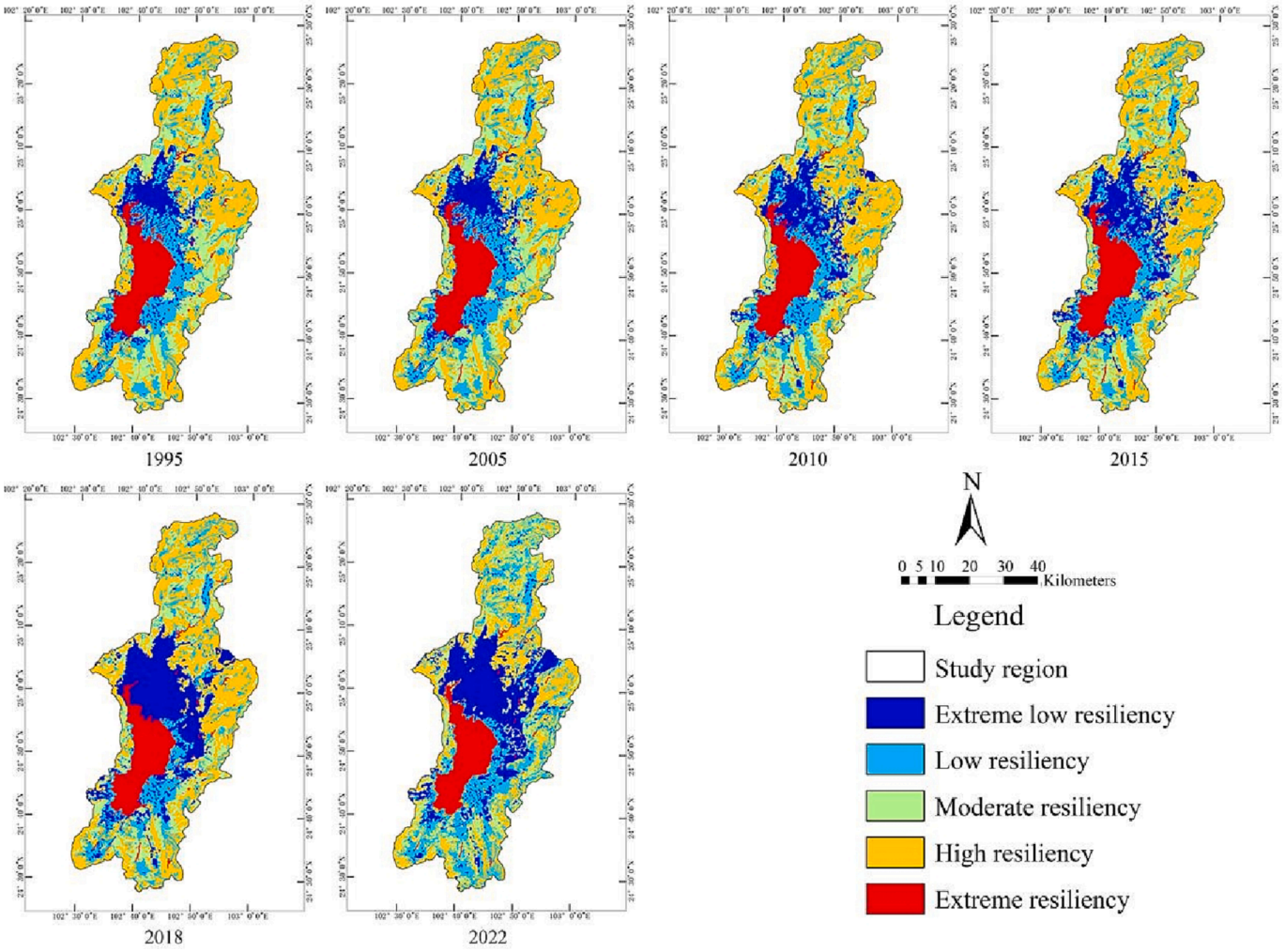

Fig. 2. LUCC resiliency of DLB from 1995 to 2022.

Table 4
NDVI resiliency of DLB from 1995 to 2022.

Region	Extreme low resiliency area		Low resiliency area		Moderate resiliency area		High resiliency area		Extreme resiliency area	
	Area/ km^2	Percentage/%	Area/ km^2	Percentage/%	Area/km^2	Percentage/%	Area/ km^2	Percentage/%	Area/km^2	Percentage/%
1995	1808.41	58.91	1123.15	36.59	137.74	4.49	0.36	0.01	0.00	0.00
2005	1510.54	49.21	1156.06	37.66	383.76	12.50	19.21	0.63	0.00	0.00
2010	1714.44	55.85	934.79	30.45	417.21	13.59	3.18	0.10	0.00	0.00
2015	1598.10	52.06	1460.98	47.59	10.59	0.35	0.00	0.00	0.00	0.00
2018	1160.84	37.82	1479.77	48.21	428.95	13.97	0.07	0.00	0.00	0.00
2022	1799.28	58.62	1263.65	41.17	6.69	0.22	0.00	0.00	0.00	0.00

2022 (Wang et al., 2022; Shooshtari et al., 2015) (Table 5, Table 6, Fig. 5). The single-factor study of landscape patterns shows that the overall LI resiliency of Dianchi watershed was high from 1995 to 2022, with the sum of highly and extremely resiliency areas accounting for more than 50%. The spatial distribution of LI resiliency is discrete, and the areas with low resiliency are mainly located in the central part of the DLB and its fringes.

4.2. Ecological resiliency evaluation of integrated factors

The evaluation results show (Table 7, Table 8 and Fig. 6) that from 1995 to 2022, the percentage of extremely high resiliency areas in DLB has remained very low and negligible. The extreme low resiliency area increased by 0.84%, the low- resiliency area increased by 6.23%, the medium-resiliency area decreased by 4.93%, and the high-resiliency area decreased by 2.14%. The spatial distribution of extreme low resiliency areas has remained mostly distributed in the middle and upper part of the basin and the fringe areas. In contrast, low-resiliency areas are distributed in the basin, and medium-resiliency areas, which account for more than 40% of the area, are scattered in the basin, while high-resiliency areas were concentrated in the basin water system and the fringe areas.

The ecological resiliency of DLB was decreasing across the time series, while the area of extreme low resiliency areas increased by more than 90% from 1995 to 2022. Simultaneously, the area of low-resiliency areas increased by 191.08 km^2, the area of medium-resiliency areas

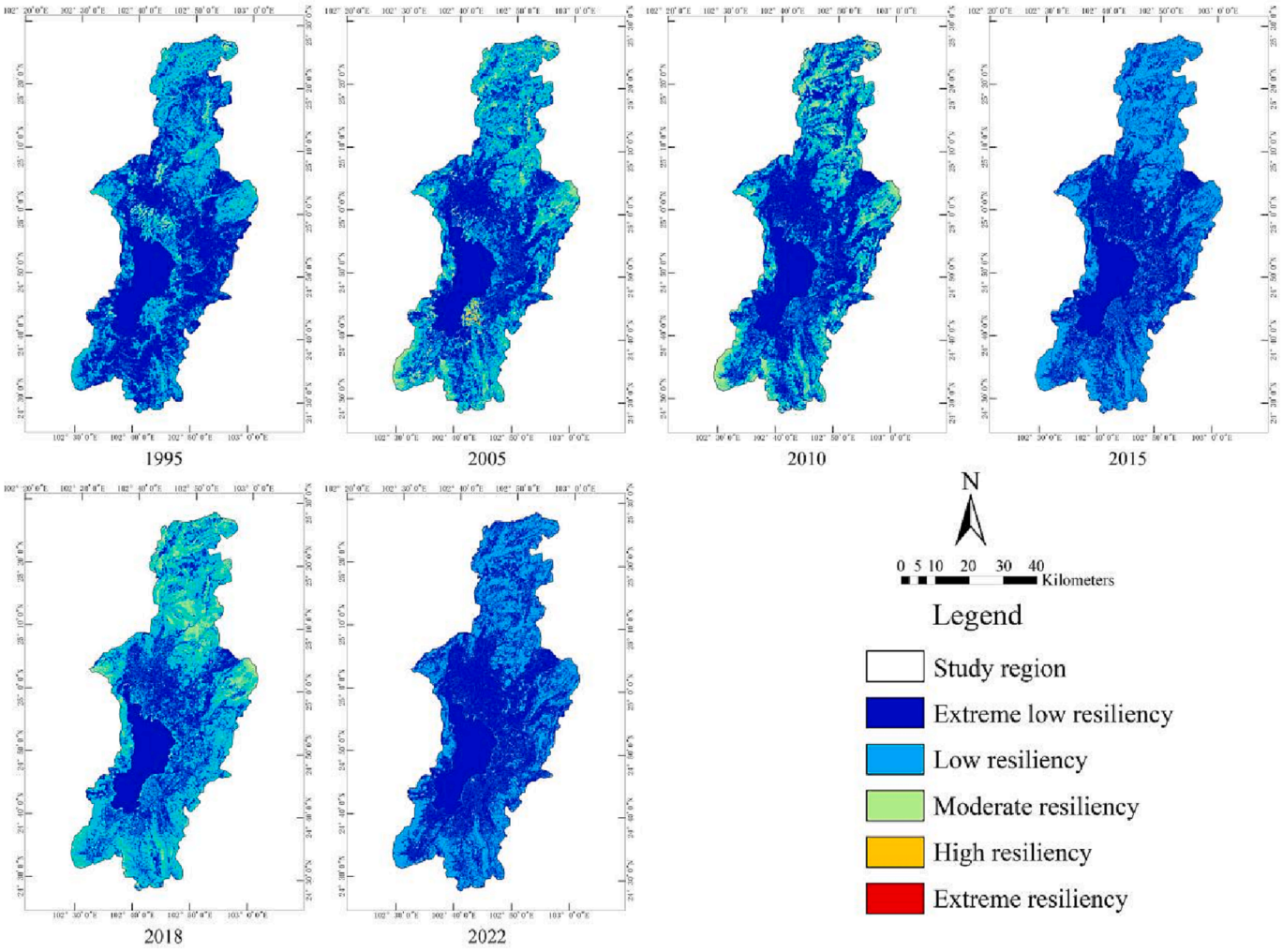

Fig. 3. NDVI resiliency of DLB from 1995 to 2018.

decreased by 151.16 km^2; the area of highly resiliency areas decreased by 65.50 km^2.

4.3. Analysis of ecological resiliency level shift of integrated factors

From 1995 to 2022, the chord diagram illustrated the ecological resiliency level shift in DLB (Fig. 7). In terms of ecological resiliency level shift, the area of extremely resilient areas remained approximately the same, while the area of the rest of ecological resiliency levels all experienced some shift. In terms of transition direction, the extreme low resiliency areas mainly transitioned to low-resiliency areas and moderate-resiliency areas. Meanwhile, the low-resiliency areas mainly transitioned to extreme low resiliency, moderate-resiliency and highly resiliency areas. The moderate-resiliency areas mainly transitioned to extreme low resiliency, low-resiliency and highly resiliency areas. Less change was seen among the highly resiliency areas. When these areas showed transformation, they mainly transitioned to low-resiliency and moderate-resiliency areas.

The analysis of the transfer of ecological resiliency level in the watershed shows that the extremely resiliency areas have less area change and are less disturbed by human activities. In contrast, areas with higher ecological resiliency levels in the watershed continue to shift to lower levels, indicating that human activities and land use changes in the study area influence ecological resiliency levels.

4.4. Ecological resiliency center of gravity migration analysis

The migration of the center of gravity of ecological resiliency areas in the DLB from 1995 to 2022 (Table 9 and Fig. 8) shows the vectorial relationship between the center of gravity and the different ecological resiliency levels. Within the six years of 1995, 2005, 2010, 2015, 2018, and 2022, each resiliency area is migrating to different degrees. The gravity migration analysis shows that different ecological resiliency areas generally show a trend of transfer to the northeast. National policies mainly influence the changes in the center of gravity of ecological resiliency resiliency areas.

4.5. Ecological resiliency kernel density estimation

The density distribution of ecological resiliency nuclei in DLB from 1995 to 2022 (Fig. 9). From the spatial distribution, the resiliencyExtreme low resiliency density nuclei were mostly distributed around Dianchi. In contrast, the low and moderate resiliency nuclei were distributed in the watershed. The highly resiliency density nuclei were mainly distributed widely across the watershed edge. Finally, the extremely high resiliency density nuclei were concentrated in the middle and upper part of the watershed. Highly resilient areas were firstly distributed in the northern, south and marginal areas of the watershed and then shifted to the margins; extremely high resiliency areas were firstly distributed in the northwestern part of the watershed and then shifted to the middle of the watershed.

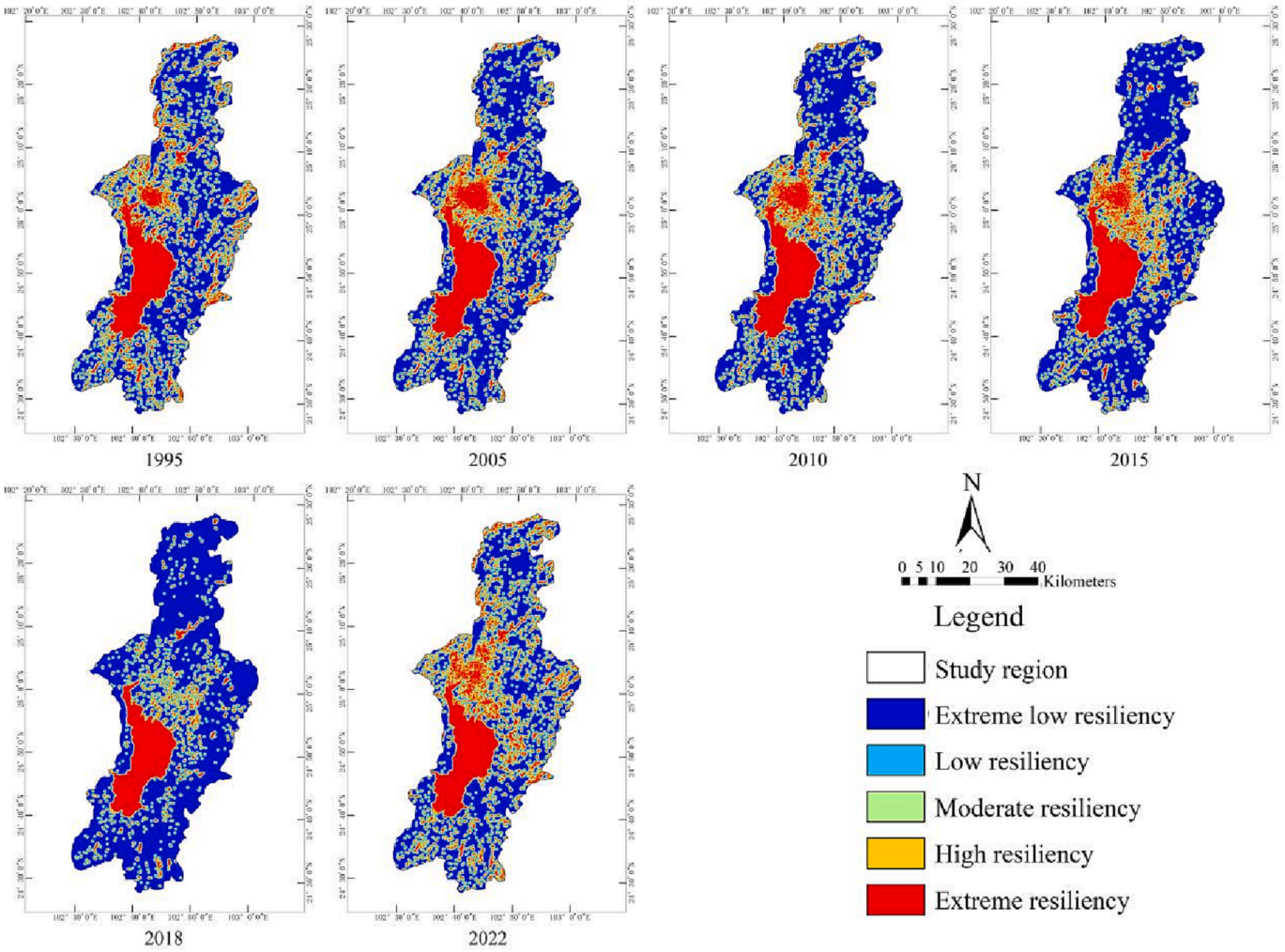

Fig. 4. RB resiliency of DLB from 1995 to 2018.

Table 5
The proportion of RB of DLB from 1995 to 2022.

Region	Extreme low resiliencyarea		Low resiliency area		Moderate resiliency area		High resiliency area		Extreme hight resiliency area	
	Area/ km^2	Percentage/%	Area/ km^2	Percentage/%	Area/ km^2	Percentage/%	Area/ km^2	Percentage/%	Area/ km^2	Percentage/%
1995	1120.73	36.51	475.26	15.48	540.58	17.61	330.33	10.76	602.80	19.64
2005	1248.23	40.69	435.26	14.19	482.91	15.74	298.46	9.73	603.16	19.67
2010	1371.44	44.68	412.70	13.44	450.87	14.69	273.27	8.90	561.43	18.29
2015	1472.35	47.97	363.35	11.84	413.61	13.47	266.85	8.69	553.46	18.03
2018	1899.24	61.87	308.02	10.03	300.49	9.79	152.56	4.97	409.58	13.34
2022	1013.18	33.00	473.14	15.41	572.57	18.65	375.63	12.23	635.01	20.69

Table 6
Landscape Indices resiliency area of DLB from 1995 to 2022.

Region	Extreme low resiliency area		Low resiliency area	Moderate resiliency area			High resiliency area		Extreme resiliency area	
	Area/ km^2	Percentage/%	Area/ km^2	Percentage/%	Area/ km^2	Percentage/%	Area/ km^2	Percentage/%	Area /km^2	Percentage/%
1995	141.35	4.61	257.15	8.38	698.04	22.75	1116.03	36.37	855.89	27.89
2005	312.30	10.18	441.18	14.38	677.71	22.09	785.49	26.50	851.81	27.76
2010	0.00	0.00	327.84	10.68	1180.71	38.46	1561.18	50.86	0.00	0.00
2015	115.26	3.76	225.26	7.34	473.61	15.43	1241.14	40.43	1014.46	33.05
2018	0.00	0.00	437.13	14.24	1074.62	35.01	1557.97	50.75	0.00	0.00
2022	82.51	2.69	232.61	7.58	421.33	13.73	1120.07	36.49	1213.25	39.52

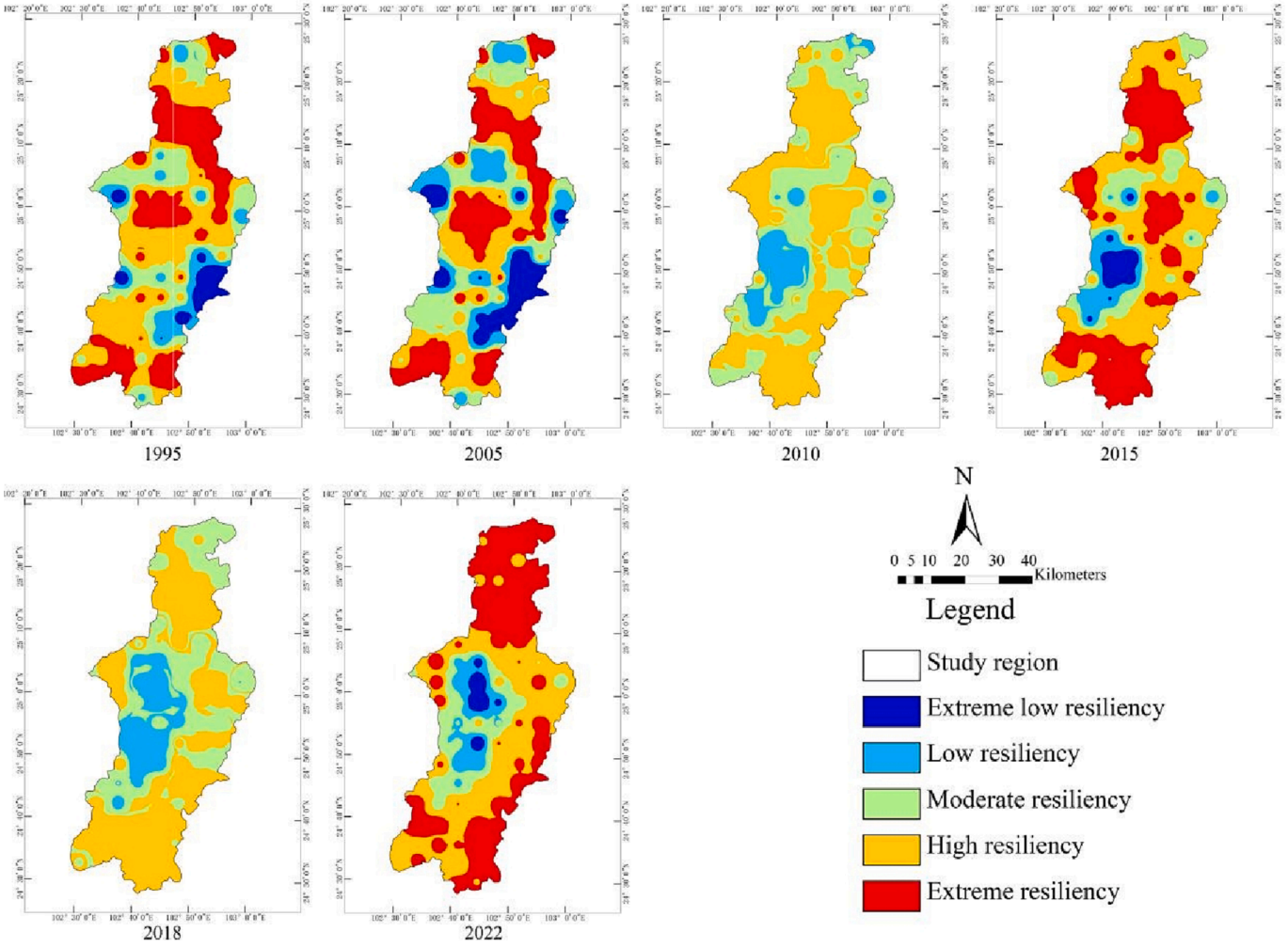

Fig. 5. Landscape Indices resiliency of DLB from 1995 to 2018.

Table 7
The factors are weighted of integrated ecological resiliency of DLB.

Grade 1	Weight	Grade 2	Weight	Grade 3	Weight
Integrated ecological resiliency of DLB	1.00	Land-use type factor	0.29	–	0.29
		Vegetation coverage factor	0.21	–	0.21
		Water buffer factor	0.28	–	0.28
		Landscape pattern factor	0.22	LPI	0.03
				AREA_MN	0.02
				SHDI	0.08
				SHEI	0.09

4.6. CA-MC model integrated ecological resiliency prediction analysis

The simulation errors in 2015 were assessed to be within 10%. The Kappa coefficients were 0.87 (5 years) and 0.82 (10 years), respectively, which showed accurate prediction results (Table 10). The CA-MC model obtained the integrated ecological resiliency distribution and the percentage of resiliency areas in 2026 and 2030 in the DLB (Table 11 and Fig. 10). The evolution pattern of resiliency areas in 2026–2030 were similar in 2022–2026. However, the overall resiliency areas level was predicted to increase. By 2026, the proportion of extreme low resiliency areas will decrease by 1.70%, shifting to low, medium, and high resiliency areas. 2026–2030, the non- and medium resiliency areas were predicted to increase by 9.51 km^2 and 9.86 km^2, respectively, while the low and high resiliency areas are predicted to decrease by 1699.95 hm^2 and 238.10 hm^2, respectively. The above phenomenon reflects 2022 and reflects that the ecological resiliency of the DLB will increase from 2022 to 2030 due to the decrease in the extreme low resiliency area and the increase in moderate resiliency.

5. Discussion

5.1. Ecological resiliency research

As this is the primary stage study to attempt multi-parameter weighting to assess temporal change in ecological resiliency in China, we recognized that the choice of indicators and their objective connection to actual functional ecological resiliency need to further improve in the future. The indexes that we chose were based on assumption what natural area with better integrity have better resiliency, while urban development and areas disturbed by human beings have reduced ecological resiliency (Lu et al., 2023; Wang et al., 2023). According to the research results, a positive aspect is that urban ecological recovery is under way, which is the seed of ecological restoration. The shortcoming is that systematic governance is also lacking.

In this study, we used a variety of methods to research the spatial and temporal evolution of ecological resiliency in the DLB in southern China. In terms of factor weight construction, this paper adopts the entropy value method and entropy weight TOPSIS to calculate the weights of the influencing factors and then processed via the weighted overlay analysis (Fu et al., 2019). Our results demonstrated that the ecological resiliency

Table 8
Ecological resiliency resiliency area of DLB from 1995 to 2022.

Region	Extreme low resiliency area		Low resiliency area		Moderate resiliency area		High resiliency area		Extreme resiliency area	
	Area/ km^2	Percentage/%	Area/ km^2	Percentage/%	Area/ km^2	Percentage/%	Area/ km^2	Percentage/%	Area/ km^2	Percentage/%
1995	28.41	0.93	1025.11	33.43	1465.86	47.80	547.07	17.84	0.26	0.01
2005	49.66	1.62	1079.60	35.20	1418.72	46.26	518.13	16.90	0.60	0.02
2010	18.42	0.60	1093.74	35.66	1499.64	48.90	454.97	14.84	0.00	0.00
2015	12.19	0.40	920.70	30.02	1709.61	55.75	424.24	13.83	0.03-	0.00
2018	118.88	3.88	1268.60	41.37	1311.63	42.77	367.61	11.99	0.00	0.00
2022	54.25	1.77	1216.19	39.66	1314.70	42.87	481.57	15.70	0.00	0.00

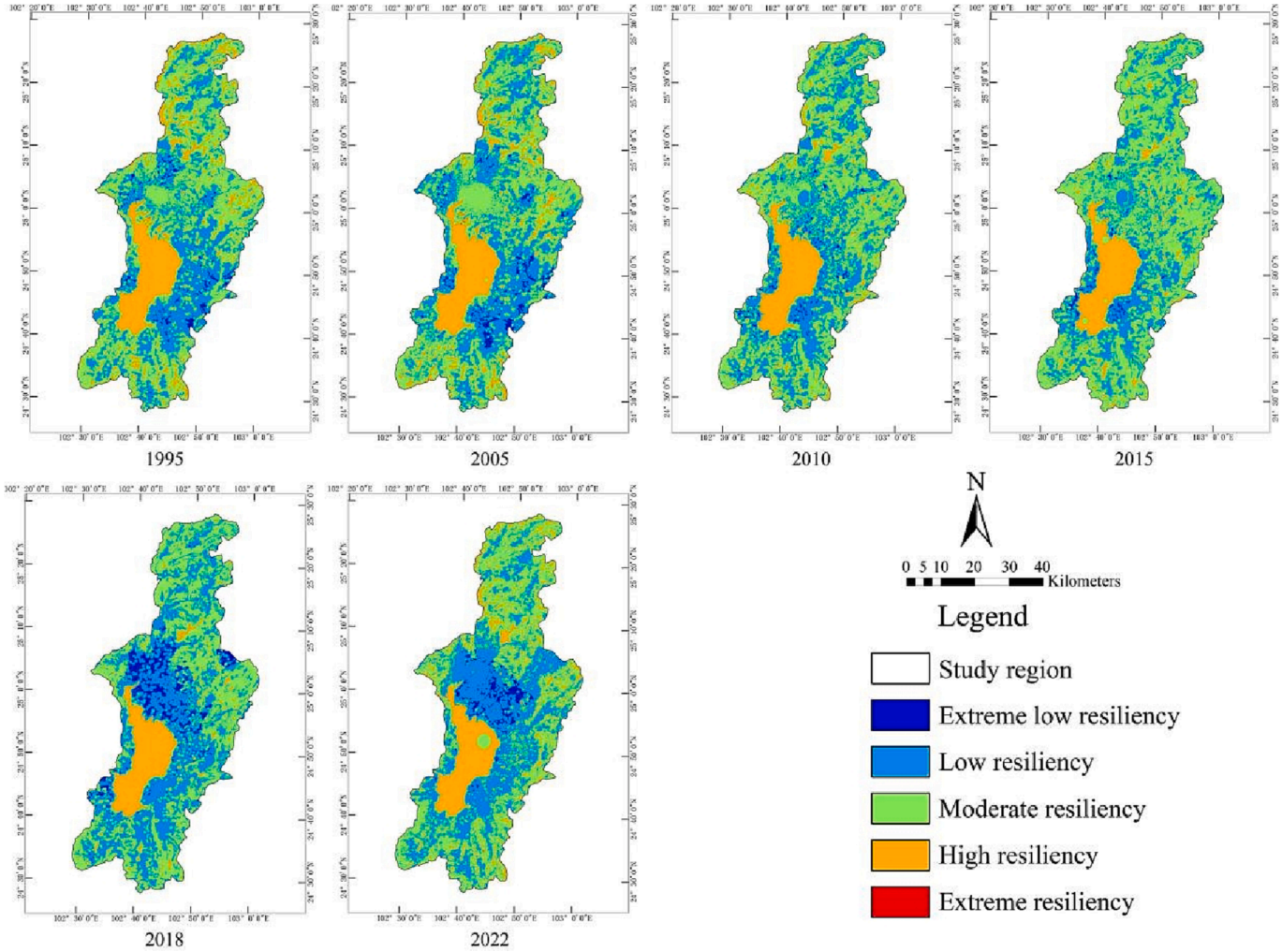

Fig. 6. Integrated ecological resiliency of DLB from 1995 to 2022.

of DLB decreasing from 1995 to 2022. These findings are similar previous studies on land use, water environment, and landscape pattern, in the DLB (Wu et al., 2022; Wang et al., 2021a; Hong et al., 2011; Wang et al., 2021b). However, these previous papers could not quantify the evolution of the ecological resiliency in DLB, because they only consider the role of a single or two factors. We selected multiple factors and used the entropy value method and entropy weight TOPSIS method to create a multi-factor weighted indicator of ecological resiliency.

The CA-MC model was used to simulate future trends in ecological resiliency and dissect the spatial evolution of ecological resiliency areas (Fu et al., 2022; Fu et al., 2018). The results showed that, compared with 2022, the predicted extreme low resiliency areas of Dianchi watershed in 2026 and 2030 decreased, while the areas of low and moderate resiliency are predicted to increase, indicating a gradual improvement in ecological resiliency; the overall rank of the ecological resiliency of the watershed in 2026 and 2030 is predicted to increase compared with that

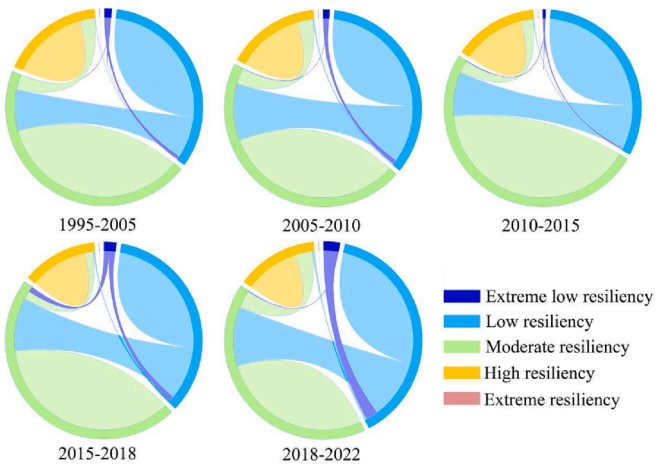

Fig. 7. Chord Diagram of ecological resiliency transfer in DLB, 1995–2022.

Table 9
The migration distance of the resiliency area gravity center from 1995 to 2022.

Region transformation distance (km)	1995	2005	2010	2015	2018	2022
Extreme low resiliency area	9.68	15.61	10.71	17.67	6.88	4.12
Low resiliency area	3.31	1.61	1.54	1.88	1.83	2.04
Moderate resiliency area	3.72	3.63	3.74	3.76	4.77	3.37
High resiliency area	4.46	6.61	8.85	10.84	12.44	5.02
Extreme resiliency area	8.00	8.42	10.27	6.28	15.08	18.61

in 2022. The extremely, high and moderately resilient areas were mainly distributed along the river system as well as forests and grasslands. In contrast, the low and non-resilient areas are mainly concentrated in the urbanized land and surrounding arable land, with a more dispersed spatial distribution.

5.2. Migration of the center of gravity of ecological resiliency areas

We found that the trend of different ecological resiliency area transfer to the northeast, which is not the result of artificial intervention, but is caused by years of change in resilient patch. Additionally, it's actually difficult to capture the trajectories of migration of the center of gravity, the trajectories are affected by many factors such as climate and national policies (Li et al., 2022; Liu et al., 2020).

5.3. Nuclear density of ecological resiliency areas

The ecological resiliency is decreasing from the core of water and woodland. The extrapolation results are similar as the findings of the ecological resiliency study of the Yanhe River basin, reflect the characteristics of the distribution of ecological resiliency levels in the plateau basin (Yang and Zhang, 2021).

5.4. CA-MC model ecological resiliency derivation

CA-MC model was initially used to simulate the future evolution trend of land use. Later it was gradually applied to landscape pattern and ecosystem services (Guan et al., 2011; Sang et al., 2011; Ye and Bai, 2007; Chu et al., 2018; Zhao et al., 2019). In this paper, we innovatively applied the CA-MC model to the evaluation of ecological resiliency. Our results show that, the extremely, the high and moderately resilient areas are mainly distributed along the river system as well as forests and grasslands. In contrast, the low and in resiliency areas are mainly concentrated in the urbanized land and surrounding arable land, with a more disperse spatial distribution which provides important theoretical guidance and a technical basis for ecological protection, urban planning and strategic land use management in DLB.

5.5. Countermeasures and recommendations

The sustainable development of the ecological environment of the basin should first ensure the integrity of the ecosystem and the comprehensive set of ecological services it provides. However, it should be noted that ecological resiliency is not an absolute attribute, but a relative one.

Through eco-restoring project, improving the single-factor of

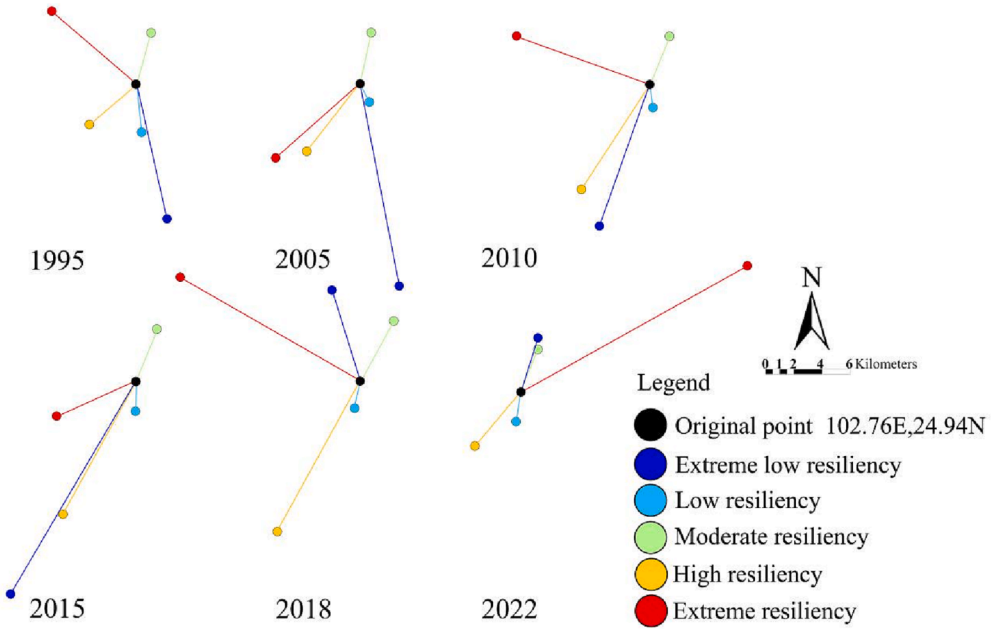

Fig. 8. The migration variety of the resiliency area gravity center from 1995 to 2022.

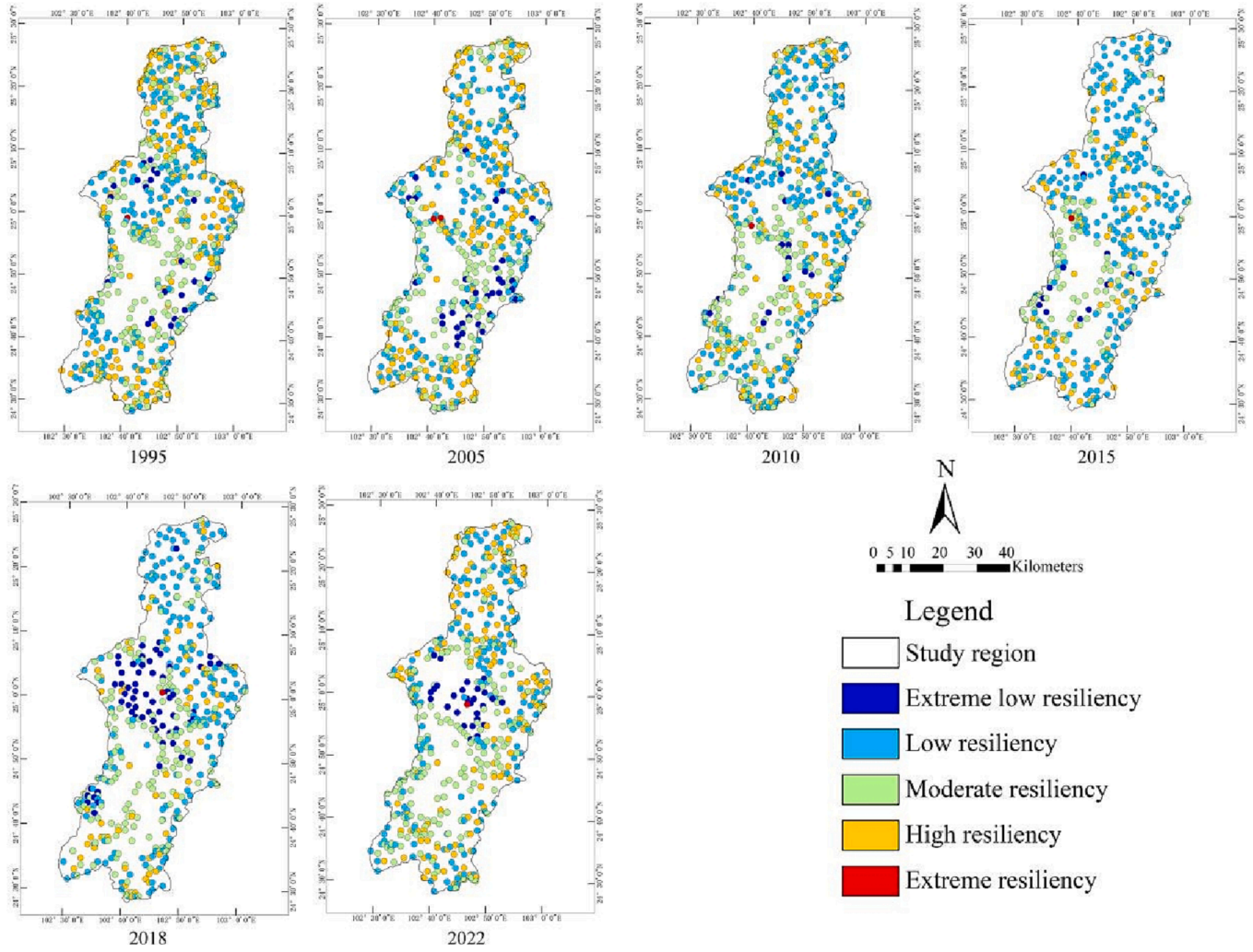

Fig. 9. Kernel density estimation of dlb from 1995 to 2022.

Table 10
Ecological resiliency simulation accuracy of DLB in 2015.

Grade of resiliency area	2015 (5 years) area/hm^2	2015 (10 years) area/hm^2	2015 (Actuality) area/hm^2	Average simulation error (%)
Extreme low resiliency area	1255.10	1271.56	1218.99	3.64
Low resiliency area	93941.02	99338.60	92070.26	4.96
Moderate resiliency area	171122.77	160578.01	170961.04	3.08
High resiliency area	40368.02	45486.82	42423.70	6.03
Extremely resiliency area	3.41	3.33	3.51	4.02

ecological resiliency in our study and thereby influencing the distribution of the high level of the ecological resiliency. According to the understanding of nuclear density and center of gravity transfer, think the DLB future planning policy should let the Land use plan as the center, control the area and dispersion of extreme low resiliency, will affect landscape indices resiliency and land use resiliency. Through ecological adjustment and control the land use extreme low resiliency area can increase the forest area and water area. According to the evaluation system, decreasing the extreme low resiliency and low resiliency area of land use can increase the area of high resiliency and extreme resiliency area high resiliency area. The overall ecological resiliency will be more stable compared with the previous period, and the center of gravity transfer and nuclear density distribution will not change substantially. According to the actual situation, the DLB can be divided into four kinds of ecological areas, and corresponding control and construction opinions can be proposed according to different resiliency construction requirements (Cai et al., 2021; Yang et al., 2022; Qian et al., 2022). The extreme low resiliency areas will be prioritized for construction areas for urban renewal. The low-resiliency areas will prioritize for designation as ecological buffer zones for moderate development and green infrastructure. The moderately resiliency areas will be prioritized for ecological buffer zones and increased forest coverage. The extremely and highly resilient areas will be designated as ecological protection zones. Moreover, all construction activities unrelated to ecological protection will be prohibited. In principle, all construction activities unrelated to ecological protection are prohibited, and the area and strength of protected areas are increased.

6. Conclusion

This paper uses GIS ecological resiliency analysis combined with CA-MC model, center of gravity migration, and nuclear density analysis to scientifically reveal ecological resiliency's spatial and temporal evolution characteristics in DLB. This paper constructs indicators from four

Table 11
Variation characteristics of dlb from 2022 to 2030.

Grade of resiliency area	Predicted area in 2026	Predicted area in 2030/hm^2	2022–2026		2026–2030	
			Changed area/hm^2	Change rate/%	Changed area/hm^2	Change rate/%
Extreme low resiliency area	10640.70	9689.57	−5215.58	−1.70	951.14	0.31
Low resiliency area	116981.19	118681.14	4637.75	1.51	−1699.95	−0.55
Moderate resiliency area	130908.97	129923.07	560.59	0.18	985.90	0.32
High resiliency area	48139.05	48377.15	17.49	0.01	−238.10	−0.08
Extremely resiliency area	0.10	0.09	−0.04	0.00	0.01	0.00

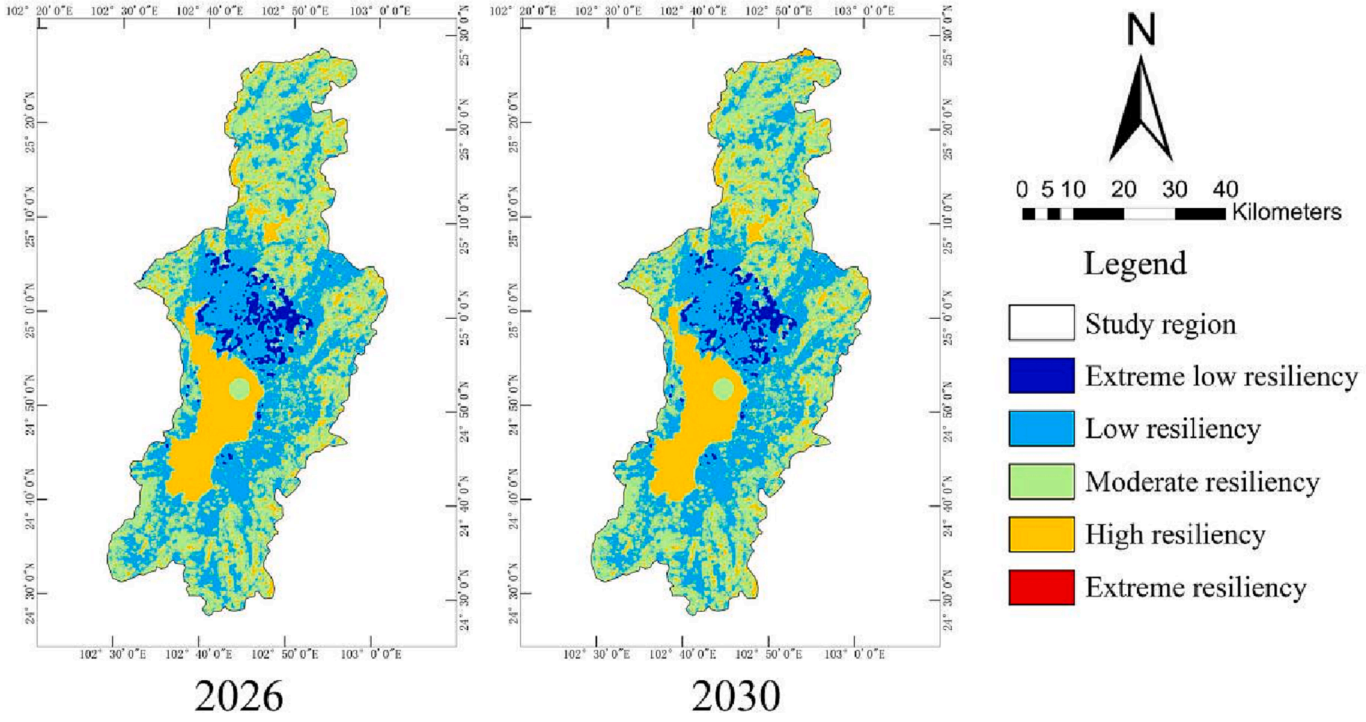

Fig. 10. Predicted integrated ecological resiliency of dlb.

aspects: LUCC, NDVI, RB, and LI. The indicators behind ecological resiliency should be considered as a priority in future ecological management. However, ecological resiliency indicators can differ between cases, so the causal relationships between these indicators and ecological resiliency should also be further addressed. Despite some limitations in the methodology and some data of results have certain degree of dispersion, this study demonstrated the mildly resilient areas shift to the northwest, and the highly resilient areas shift to the southeast in DLB from 1995 to 2022. We also quantified the degree of resiliency of the system of current and future conditions, which can proposed timely ecological protection strategies.

Funding

This research was funded by Yunnan Province Education Department, China, No.2020J0274; Awarded a scholarship by the China Scholarship Council (CSC) in 2022, file No.202208535037. Yunnan Agricultural University Research Start-up Fund Project No. KY2019-28.

Declaration of Competing Interest

The authors declare that they have no known competing financial interests or personal relationships that could have appeared to influence the work reported in this paper.

Data availability

Data will be made available on request.

Acknowledgements

We thank professor Zhang Jingli, College of Horticulture and Landscape, Yunnan Agricultural University, offered suggestions for modification. Although the study involved evolution of ecological integrity, it has not been implemented in actual construction and is still in the research stage. Consequently, the views, interpretations, and conclusions expressed in this article are solely those of the authors and do not necessarily reflect or represent local government views or policies.

Institutional review board statement

Not applicable.

Informed consent statement

We would like to emphasize that participation in this research is entirely voluntary, and you have the right to withdraw your consent at any time. This study is conducted for public welfare purposes and aims to provide a scientific analysis for the preservation of the landscape ecology in the Dianchi Lake Basin.The corresponding author, Dr. Tian Bai, provided the primary and most significant guidance for this paper.

This research is part of Tian Bai's research team, with Dr. Yawen Wu. The first authors completed the paper under the careful guidance of the two aforementioned researchers. The research team will continue to focus on studying the landscape ecological changes in the Yunnan Plateau lake basins. The copyright of the paper belongs to Dr. Tian Bai's research team.

References

Aburas, M.M., Ho, Y.M., Ramli, M.F., Ash'aari, Z.H., 2017. Improving the capability of an integrated CA-Markov model to simulate spatio-temporal urban growth trends using an Analytical Hierarchy Process and Frequency Ratio. Int. J. Appl. Earth Obs. Geoinf. 59, 65–78. https://doi.org/10.1016/j.jag.2017.03.006.

Adhikari, S., Southworth, J., 2012. Simulating Forest Cover Changes of Bannerghatta National Park Based on a CA-Markov Model: A remote sensing approach. Remote Sens. (Basel) 4 (10), 3215–3243. https://doi.org/10.3390/rs4103215.

Amiri, V., Rezaei, M., Sohrabi, N., 2014. Groundwater quality assessment using entropy weighted water quality index (EWQI) in Lenjanat, Iran. *Environ. Earth Sci.* 72 (9), 3479–3490. https://doi.org/10.1007/s12665-014-3255-0.

Baqa, M.F., Chen, F., Lu, L., Qureshi, S., Tariq, A., Wang, S., Jing, L., Hamza, S., Li, Q., 2021. Monitoring and modeling the patterns and trends of urban growth using urban sprawl matrix and CA-Markov model: A case study of Karachi, Pakistan. *Land* 10 (7), 700. https://doi.org/10.3390/land10070700.

Bigot, J., Klein, T., 2012. Consistent estimation of a population barycenter in the Wasserstein space. ArXiv e-prints, 49. https://doi.org/10.48550/arXiv.1212.2562.

Cai, X., Li, Z., Liang, Y., 2021. Tempo-spatial changes of ecological vulnerability in the arid area based on ordered weighted average model. Ecol. Ind. 133, 108398 https://doi.org/10.1016/j.ecolind.2021.108398.

Chambers, J.C., Allen, C.R., Cushman, S.A., 2019. Operationalizing ecological resiliency concepts for managing species and ecosystems at risk. Front. Ecol. Evol. 7, 241. https://doi.org/10.3389/fevo.2019.00241.

Chang M.E., Zhao Zhi Qing,Chang Hsiao Tung & Shu Bo. 2021.Urban green infrastructure health assessment, based on landsat 8 remote sensing and entropy landscape metrics. European Journal of Remote Sensing (1).54, 417-430. doi: 10.1080/22797254.2021.1948357.

Chen, J., Wu, C., 2020. Evaluation of ecological sensitivity in Erhai Lake Basin, southwest China. IOP Conference Series: Earth and Environmental Science 612 (1), 012072. https://doi.org/10.1088/1755-1315/612/1/012072.

Cheng, W., Haiyang, X., Celestin, S., Jianhua, S., Chenguang, Z., Tengfei, Y., Tuanrong, W., 2020. Ecosystem health assessment of desert nature reserve with entropy weight and fuzzy mathematics methods: A case study of Badain Jaran Desert. Ecological Indicators 119. https://doi.org/10.1016/j.ecolind.2020.106843.

Chi, Y., Zhang, Z., Gao, J., Xie, Z., Zhao, M., Wang, E., 2019. Evaluating landscape ecological sensitivity of an estuarine island based on landscape pattern across temporal and spatial scales. Ecol. Ind. 101, 221–237. https://doi.org/10.1016/j.ecolind.2019.01.012.

Chow, T.E., Sadler, R., 2010. The consensus of local stakeholders and outside experts in suitability modeling for future camp development. Landsc. Urban Plan. 94 (1), 9–19. https://doi.org/10.1016/j.landurbplan.2009.07.013.

Chu, L., Sun, T., Wang, T., Li, Z., Cai, C., 2018. Evolution and prediction of landscape pattern and habitat quality based on CA-Markov and InVEST model in Hubei section of Three Gorges Reservoir Area (TGRA). Sustainability 10 (11), 3854. https://doi.org/10.3390/su10113854.

Civco, D.L., 1993. Artificial neural networks for land-cover classification and mapping. Int. J. Geogr. Inf. Syst. 7 (2), 173–186. https://doi.org/10.1080/02693799308901949.

Cui, L., Zhao, Y., Liu, J., Wang, H., Han, L., Li, J., Sun, Z., 2021. Vegetation Coverage Prediction for the Qinling Mountains Using the CA–Markov Model. ISPRS Int. J. Geo Inf. 10 (10), 679. https://doi.org/10.3390/ijgi10100679.

Cushman, S.A., McGarigal, K., 2019. Metrics and models for quantifying ecological resiliency at landscape scales. Front. Ecol. Evol. 7, 440. https://doi.org/10.3389/fevo.2019.00440.

Deng, L., Zhang, Q., Cheng, Y., Cao, Q., Wang, Z., Wu, Q., Qiao, J., 2022. Underlying the influencing factors behind the heterogeneous change of urban landscape patterns since 1990: A multiple dimension analysis. Ecol. Ind. 140, 108967 https://doi.org/10.1016/j.ecolind.2022.108967.

Duan, Z., Wang, M., Liu, Y., Gao, W., Chang, X., 2021b. Predicting hydrological alterations to quantitative and localized climate change in plateau regions: A case study of the Lake Dianchi Basin, China. Stoch. Env. Res. Risk A. 36 (4), 969–983. https://doi.org/10.1007/s00477-021-02126-6.

Duan, X., Zou, H., Wang, L., Chen, W., Min, M., 2021a. Assessing ecological sensitivity and economic potentials and regulation zoning of the riverfront development along the Yangtze River, China. *J. Clean. Prod.* 291, 125963 https://doi.org/10.1016/j.jclepro.2021.125963.

Elgammal, A., Duraiswami, R., Harwood, D., Davis, L., 2002. Background and foreground modeling using nonparametric kernel density estimation for visual surveillance. Proc. IEEE 90 (7), 1151–1163. https://doi.org/10.1109/jproc.2002.801448.

Fu, F., Deng, S., Wu, D., Liu, W., Bai, Z., 2022. Research on the spatiotemporal evolution of land use landscape pattern in a county area based on CA-Markov model. Sustain. Cities Soc. 80, 103760 https://doi.org/10.1016/j.scs.2022.103760.

Fu, M., Tian, J., Ren, Y., Li, J., Liu, W., Zhu, Y., 2019. Functional zoning and space management of three-river-source national park. J. Geog. Sci. 29, 2069–2084. https://doi.org/10.1007/s11442-019-1705-z.

Fu, X., Wang, X., Yang, Y.J., 2018. Deriving suitability factors for CA-Markov land use simulation model based on local historical data. J. Environ. Manage. 206, 10–19. https://doi.org/10.1016/j.jenvman.2017.10.012.

Gatrell, A.C., Bailey, T.C., 1996. Interactive spatial data analysis in medical geography. Soc. Sci. Med. 42 (6), 843–855.

Guan, D., Li, H., Inohae, T., Su, W., Nagaie, T., Hokao, K., 2011. Modeling urban land use change by the integration of cellular automaton and Markov model. Ecol. Model. 222 (20–22), 3761–3772. https://doi.org/10.1016/j.ecolmodel.2011.09.009.

Han, B., Liu, H., Wang, R., 2015. Urban ecological security assessment for cities in the Beijing–Tianjin–Hebei metropolitan region based on fuzzy and entropy methods. Ecol. Model. 318, 217–225. https://doi.org/10.1016/j.ecolmodel.2014.12.015.

Hong, Z., Hailin, L., Zhen, C., 2011. Analysis of land use dynamic change and its impact on the water environment in Yunnan Plateau Lake Area—A Case Study of the Dianchi Lake Drainage Area. Procedia Environ. Sci. 10, 2709–2717. https://doi.org/10.1016/j.proenv.2011.09.421.

Hou, Y., Li, B., Müller, F., Chen, W., 2016. Ecosystem services of human-dominated watersheds and land use influences: a case study from the Dianchi Lake watershed in China. Environ. Monit. Assess. 188 (12), 652. https://doi.org/10.1007/s10661-016-5629-0.

Hu C., Wu Wu,Zhou Xuexia & Wang Zhijie.2023.Spatiotemporal changes in landscape patterns in karst mountainous regions based on the optimal landscape scale: A case study of Guiyang City in Guizhou Province, China. Ecological Indicators. doi: 10.1016/J.ECOLIND.2023.110211.

Huang, X., Wen, D., Li, J., Qin, R., 2017. Multi-level monitoring of subtle urban changes for the megacities of China using high-resolution multi-view satellite imagery. Remote Sensing of Environment. 196, 75. https://doi.org/10.1016/j.rse.2017.05.001.

Huang, B., Xiaoman, L., Wenwen, S., Xuejun, P., 2014. Occurrence, removal, and fate of progestogens, androgens, estrogens, and phenols in six sewage treatment plants around Dianchi Lake in China. Environmental science and pollution research international 22 (21), 12898–12908. https://doi.org/10.1007/s11356-014-3236-6.

Hwang, C.L. & Yoon, K. 1981. Multi-attribute decision: methods and applications. Springer Press, New York.

Jin, X., Wei, L., Wang, Y., Lu, Y., 2020. Construction of ecological security pattern based on the importance of ecosystem service functions and ecological sensitivity assessment: a case study in Fengxian County of Jiangsu Province, China. Environ. Dev. Sustain. 23 (1), 563–590. https://doi.org/10.1007/s10668-020-00596-2.

Kazanci Caner, Ma Qianqian, Basheer Aladeen Al, Azizi Asma. Resiliency, indirect effects and cycling in ecological networks. Ecol. Modell., 2023, 481. https://doi.org/10.1016/j.ecolmodel.2023.110346.

Li, G., Duan, W., 2015. Ecological Sensitivity Analysis of Lijiang River Based on GIS and RS. Advanced Science, Engineering and Medicine 1 (7), 81–86. https://doi.org/10.1166/asem.2015.1652.

Li, X., Janssen, A.B., de Klein, J.J., Kroeze, C., Strokal, M., Ma, L., Zheng, Y., 2019a. Modeling nutrients in Lake Dianchi (China) and its watershed. Agric. Water Manag. 212, 48–59. https://doi.org/10.1016/j.agwat.2018.08.023.

Li, H., Lu, J., Yu, J., Wu, X., Tahir, M.S., Xing, L., 2021. Identification and assessment of ecological sensitivity in Chishui River basin based on GIS. E3S Web of Conferences 267, 01016.

Li, Z.Y., Wei, W., Zhou, L., Guo, Z.C., Xie, B.B., Zhou, J.J., 2019b. Temporal and spatial evolution of ecological sensitivity in arid inland river basins of northwest China based on spatial distance index: a case study of Shiyang River Basin. Acta Ecol. Sin. 39 (20), 7463–7475. https://doi.org/10.5846/stxb201902250347.

Li, X., Zulkar, H., Wang, D., Zhao, T., Xu, W., 2022. Changes in vegetation coverage and migration characteristics of center of gravity in the Arid Desert Region of Northwest China in 30 recent years. Land 11 (10), 1688. https://doi.org/10.3390/land11101688.

Liu, S., Ye, Y., Zhong, S., 2020. Research on shift route of gravity center and decoupling relationship between urban land expansion and economic growth in China. Resources and Environment in the Yangtze Basin, 29,2563-2571. https://doi.org/10.11870 /cjlyzyyhj202012001.

Liu, H.L., Willems, P., Bao, A.M., Wang, L., Chen, X., 2016. Effect of climate change on the vulnerability of a socio-ecological system in an arid area. Global Planet. Change 137, 1–9. https://doi.org/10.1016/j.gloplacha.2015.12.014.

Lu, P., Haowei, W., Zhihui, L., 2023. Spatial-Temporal Evolutions of Ecological Environment Quality and Ecological Resiliency Pattern in the Middle and Lower Reaches of the Yangtze River Economic Belt. Remote Sens. (Basel) 15 (2). https://doi.org/10.3390/rs15020430.

Lu, C., Shi Lei, F., Lihua, L.S., Jianqiao, L., Zhenchun, M., 2023. Urban ecological environment quality evaluation and territorial spatial planning response: application to Changsha, Central China. Int. J. Environ. Res. Public Health 20 (4), 3753. https://doi.org/10.3390/IJERPH20043753.

Lu, M., Xiao-Nan, L., Yong-Hua, W., Guo-Heng, L., 2019. Ecological pattern of urban forest landscape of Ji'nan City, China. J. Appl. Ecol. 30 (12), 4117–4126. https://doi.org/10.13287/j.1001-9332.201912.017.

Luo, Y., Zhao, Y., Yang, K., Chen, K., Pan, M., Zhou, X., 2018. Dianchi Lake watershed impervious surface area dynamics and their impact on lake water quality from 1988 to 2017. Environ. Sci. Pollut. Res. 25 (29), 29643–29653. https://doi.org/10.1007/s11356-018-2967-1.

Ma, Y., Wang, Z., Li, N., Chen, J., Dhanasekaran, R., 2022. Conservation and development of residential-type historical and cultural blocks in Guangzhou under subjective evaluation. Int. Trans. Electr. Energy Syst. 2022, 1–13.

Ma, R., Yang, G., Chen, W., Zhu, H., 2004. Assessment and quantitative acquirement of factors for evaluating bank resources of the yangtze river in jiangsu province. J. Nat. Resour. 19 (2), 176–182. https://doi.org/10.1007/BF02873097.

McGarigal, K. 2014. Landscape Pattern Metrics. Wiley StatsRef: Statistics Reference Online. https://doi.org/10.1002/9781118445112.stat07723.

Mokarram, M., Pourghasemi, H.R., Hu, M., Zhang, H., 2021. Determining and forecasting drought susceptibility in southwestern Iran using multi-criteria decision-making (MCDM) coupled with CA-Markov model. Sci. Total Environ. 781, 146703 https://doi.org/10.1016/j.scitotenv.2021.146703.

Mondal, M.S., Sharma, N., Garg, P., Kappas, M., 2016. Statistical independence test and validation of CA Markov land use land cover (LULC) prediction results, Egypt. J. Remote Sens. Space Sci. 19 (2), 259–272. https://doi.org/10.1016/j.ejrs.2016.08.001.

Niu, X.Y., Wang, Y.H., Yang, H., Zheng, J.W., Zou, J., Xu, M.N., Wu, S.S., Xie, B., 2015. Effect of Land Use on Soil Erosion and Nutrients in Dianchi Lake Watershed, China. *Pedosphere* 25 (1), 103–111. https://doi.org/10.1016/s1002-0160(14)60080-1.

Qian, Y., Dong, Z., Yan, Y., Tang, L., 2022. Ecological risk assessment models for simulating impacts of land use and landscape pattern on ecosystem services. Sci. Total Environ. 833, 155218 https://doi.org/10.1016/j.scitotenv.2022.155218.

Qiao, J., Xingzhi, Y., Shuran, L., 2021. Natural language processing using neighbour entropy-based segmentation. J. Comput. Inf. Technol. 29 (2), 113–131. https://doi.org/10.20532/CIT.2021.1005393.

Sang, L., Zhang, C., Yang, J., Zhu, D., Yun, W., 2011. Simulation of land use spatial pattern of towns and villages based on CA–Markov model. Math. Comput. Model. 54 (3–4), 938–943. https://doi.org/10.1016/j.ecolmodel.2011.09.009.

Shi, Y., Li, J., Xie, M., 2018. Evaluation of the ecological sensitivity and security of tidal flats in Shanghai. Ecol. Ind. 85, 729–741. https://doi.org/10.1016/j.ecolind.2017.11.033.

Shooshtari, S.J., Gholamalifard, M., 2015. Scenario-based land cover change modeling and its implications for landscape pattern analysis in the Neka Watershed, Iran. Remote Sensing Applications: Society and Environment 1, 1–19. https://doi.org/10.1016/j.rsase.2015.05.001.

Silverman, B.W., 1986. Density estimation for statistics and data analysis. Monogr. Statist. Appl. Probab. https://doi.org/10.1201/9781315140919.

Souidi, H., Ouadif, L., Bahi, L., Habitou, N., 2019. Spatiotemporal Monitoring and Prediction of Land Use Integrating the Markov Chain and Cellular Automata in the Coastal Chaouia. Int. J. Recent Technol. Eng. (IJRTE) (4).

Wang, R., Bai, Y., Alatalo, J.M., Yang, Z., Yang, Z., Yang, W., Guo, G., 2021a. Impacts of rapid urbanization on ecosystem services under different scenarios – A case study in Dianchi Lake Basin, China. *Ecol. Ind.* 130, 108102 https://doi.org/10.1016/j.ecolind.2021.108102.

Wang, X.L., Blanchet, F.G., Koper, N., 2014. Measuring habitat fragmentation: An evaluation of landscape pattern. Methods Ecol. Evol. 5 (7).

Wang, Y., Cai, Y., Xie, Y., Chen, L., Zhang, P., 2023. An integrated approach for evaluating dynamics of urban eco-resiliency in urban agglomerations of China. Ecol. Ind. 146 https://doi.org/10.1016/j.ecolind.2023.109859.

Wang, R., Xu, X., Bai, Y., Alatalo, J.M., Yang, Z., Yang, W., Yang, Z., 2021b. Impacts of urban land use changes on ecosystem services in Dianchi Lake Basin, China. *Sustainability* 13 (9), 4813.

Wang, Q., Yang, K., Li, L., Zhu, Y., 2022. Assessing the Terrain Gradient Effect of Landscape Ecological Risk in the Dianchi Lake Basin of China Using Geo-Information Tupu Method. Int. J. Environ. Res. Public Health 19 (15), 9634. https://doi.org/10.3390/ijerph19159634.

Wang, J., Zhang, Z., Liu, Y., 2018. Spatial shifts in grain production increases in China and implications for food security. Land Use Policy 74, 204–213. https://doi.org/10.1016/j.landusepol.2017.11.037.

Wei Xingtao, Eboy Oliver Valentine, Xu Lu, Yu Di. Ecological Sensitivity of Urban Agglomeration in the Guanzhong Plain, China. Sustainability, 2023, 15(6). https://doi.org/10.3390/su15064804.

Wen M, Zhang Ting, Li Long, Chen Longqian, Hu Sai, Wang Jia & Yuan Lina, 2021. Assessment of Land Ecological Security and Analysis of Influencing Factors in Chaohu Lake Basin, China from 1998–2018. Sustainability (1). 13, 358. doi: 10.3390/SU13010358.

Wu, Q., Yang, R., Yang, Z., 2022. A study on the rationality of land use change in the Dianchi Basin during the last 40 years under the background of lake revolution. Sustainability 14 (18), 11479. https://doi.org/10.3390/su141811479.

Xie, Z., Yan, J., 2008. Kernel Density Estimation of traffic accidents in a network space. Comput. Environ. Urban Syst. 32 (5), 396–406. https://doi.org/10.1016/j.compenvurbsys.2008.05.001.

Xu, J., Ren, Q., Ziqi, Z., Wei, L., Qinglin, Y., He, C., 2021. Research on classification and hierarchical management of industrial data based on entropy Method-TOPSIS theory. Journal of Physics: Conference Series (1). https://doi.org/10.1088/1742-6596/2005/1/012001.

Yang, Y., Zhang, Y., 2021. Temporal-spatial evolutionary characteristics of ecological sensitivity in Yanhe River basin based on spatial distance index. Remote Sensing Land Resources 33 (3), 229–237. https://doi.org/10.6046/zrzyyg.2020281.

Yang, D., Zhang, P., Jiang, L., Zhang, Y., Liu, Z., Rong, T., 2022. Spatial change and scale dependence of built-up land expansion and landscape pattern evolution—Case study of affected area of the lower Yellow River. Ecol. Ind. 141, 109123 https://doi.org/10.1016/j.ecolind.2022.109123.

Ye, B., Bai, Z., 2007. Simulating land use/cover changes of Nenjiang County based on CA-Markov model. In: International conference on computer and computing technologies in agriculture. Springer, Boston, MA, pp. 321–329. https://doi.org/10.1007/978-0-387-77251-635.

Yin, Y., Zhang, D., Zhen, M., Jing, W., Luo, W., Feng, W., 2022. Combined effects of the thermal-acoustic environment on subjective evaluations in outdoor public spaces. Sustain. Cities Soc. 77, 103522.

Yu, J., Li, F., Wang, Y., Lin, Y., Peng, Z., Cheng, K., 2020. Spatiotemporal evolution of tropical forest degradation and its impact on ecological sensitivity: A case study in Jinghong, Xishuangbanna, China. *Sci. Total Environ.* 727, 138678 https://doi.org/10.1016/j.scitotenv.2020.138678.

Zhang, X., 2009. Entropy weight theory-based integrated evaluation model of natural disasters. J. Nat. Disasters 18 (6), 189–192. https://doi.org/10.13577/j.jnd.2009.063.

Zhang, M., Haijiang, J., Desuo, C., Chunbo, J., 2010. The comparative study on the ecological sensitivity analysis in Huixian karst wetland. China. Procedia Env. Sci. 2, 386–398. https://doi.org/10.1016/j.proenv.2010.10.043.

Zhang, M., Haijiang, J., Desuo, C., Chunbo, J., 2010. The comparative study on the ecological sensitivity analysis in Huixian karst wetland, China. Procedia Environ. Sci. 2, 386–398. https://doi.org/10.1016/j.proenv.2010.10.043.

Zhang, T., Zeng, W.H., Wang, S.R., Ni, Z.K., 2014. Temporal and spatial changes of water quality and management strategies of Dianchi Lake in southwest China. Hydrol. Earth Syst. Sci. 18 (4), 1493–1502. https://doi.org/10.5194/hess-18-1493-2014.

Zhang, Y., Zhang, J., Yang, Z., Li, J., 2012. Analysis of the distribution and evolution of energy supply and demand centers of gravity in China. Energy Policy 49, 695–706. https://doi.org/10.1016/j.enpol.2012.07.012.

Zhao, M., He, Z., Du, J., Chen, L., Lin, P., Fang, S., 2019. Assessing the effects of ecological engineering on carbon storage by linking the CA-Markov and InVEST models. Ecol. Ind. 98, 29–38. https://doi.org/10.1016/j.ecolind.2018.10.052.

Zhao, X., Huang, G., 2022. Urban watershed ecosystem health assessment and ecological management zoning based on landscape pattern and SWMM simulation: A case study of Yangmei River Basin. Environ. Impact Assess. Rev. 95, 106794 https://doi.org/10.1016/j.eiar.2022.106794.

Zhou, Z., Li, J., 2015. The correlation analysis on the landscape pattern index and hydrological processes in the Yanhe watershed, China. J. Hydrol. 524, 417–426. https://doi.org/10.1016/j.jhydrol.2015.02.028.

ZiębaKulawik, K., Piotr, W., 2022. Monitoring 3D Changes in urban forests using landscape metrics analyses based on multi-temporal remote sensing data. Land 11 (6), 883. https://doi.org/10.3390/LAND11060883.

Zou, T., Chang, Y., Chen, P., Liu, J., 2021. Spatial-temporal variations of ecological vulnerability in Jilin Province (China), 2000 to 2018. Ecol. Ind. 133, 108429 https://doi.org/10.1016/j.ecolind.2021.108429.

Zou, Z.H., Yi, Y., Sun, J.N., 2006. Entropy method for determination of weight of evaluating indicators in fuzzy synthetic evaluation for water quality assessment. J. Environ. Sci. 18 (5), 1020–1023. https://doi.org/10.1016/S1001-0742(06)60032-6resiliencyresiliencyResiliencyresiliency.